Available Computational Techniques to Model Atherosclerotic Plaque Progression Implementing a Multi-Level Approach

Antonis I. Sakellarios, Georgia Karanasiou, Panagiotis Siogkas, Vasiliki Kigka, Themis Exarchos, George Rigas, Lampros K. Michalis, and Dimitrios I. Fotiadis

1   Introduction

Cardiovascular disease, and more specifically atherosclerosis, is considered as one of the most common causes of death in western societies. Atherosclerosis development initiates under the effect of several conditions such as the hemodynamics environment or the rapid accumulation of lipids and their oxidation. Nevertheless, atherosclerosis is characterized as an inflammatory disease which starts after the oxidation of low density lipoproteins (LDL) into the arterial wall and the migration of monocytes and macrophages at the lesion site [1]. Blood flow and especially low endothelial shear stress (ESS) and recirculations may cause injuries in the arterial wall [2]. These regions are usually located near bifurcations, curves, and branches. It has been shown that ESS affects in different ways the endothelial function altering the local gene expression and/or the permeability to molecules [2]. This affects endothelial permeability to LDL molecules and increases LDL accumulation in the arterial wall [3]. In high risk patients, an invasive treatment is followed, such as arterial bypass or Percutaneous Coronary Intervention. In coronary artery bypass grafting (CABG), arterial or vein conduits (grafts) are used to bypass the occluded arterial region. Stenting is a combination of angioplasty and stent implantation,

A.I. Sakellarios • G. Karanasiou • P. Siogkas • V. Kigka • T. Exarchos
G. Rigas • D.I. Fotiadis (✉)
Unit of Medical Technology and Intelligent Information Systems, Department of Materials Science and Engineering, University of Ioannina, Ioannina, Greece

A.I. Sakellarios • G. Karanasiou • P. Siogkas • V. Kigka • T. Exarchos • G. Rigas • D.I. Fotiadis
Department of Biomedical Research, Institute of Molecular Biology and Biotechnology – FORTH, University Campus of Ioannina, Ioannina, Greece
e-mail: fotiadis@cc.uoi.gr

L.K. Michalis
Department of Cardiology, Medical School, University of Ioannina, Ioannina, Greece

where the tubular wire mesh is positioned in the stenosed arterial region, inflated and permanently left in order to prevent arterial recoil and restenosis. The evolution of stents has resulted in improved clinical outcomes, however, there are still some issues that should be taken into consideration, such as the induced local arterial injury, the possibility of in-stent restenosis (ISR), as well as the risk for stent thrombosis (ST) [4].

Image processing algorithms and methodologies have been implemented for the accurate reconstruction of arteries and computational models have been employed utilizing the reconstructed arterial segments or trees. In the next sections a multi-level modeling approach is presented (Fig. 1). More specifically, the first level regards the arterial reconstruction using the available invasive and non-invasive vascular imaging modalities such as intravascular ultrasound, angiography, computed tomography, and magnetic resonance imaging. The second level is the modeling of blood flow and the estimation of ESS at the reconstructed arteries. The third level is the modeling of LDL and other molecules and cells in the arterial lumen
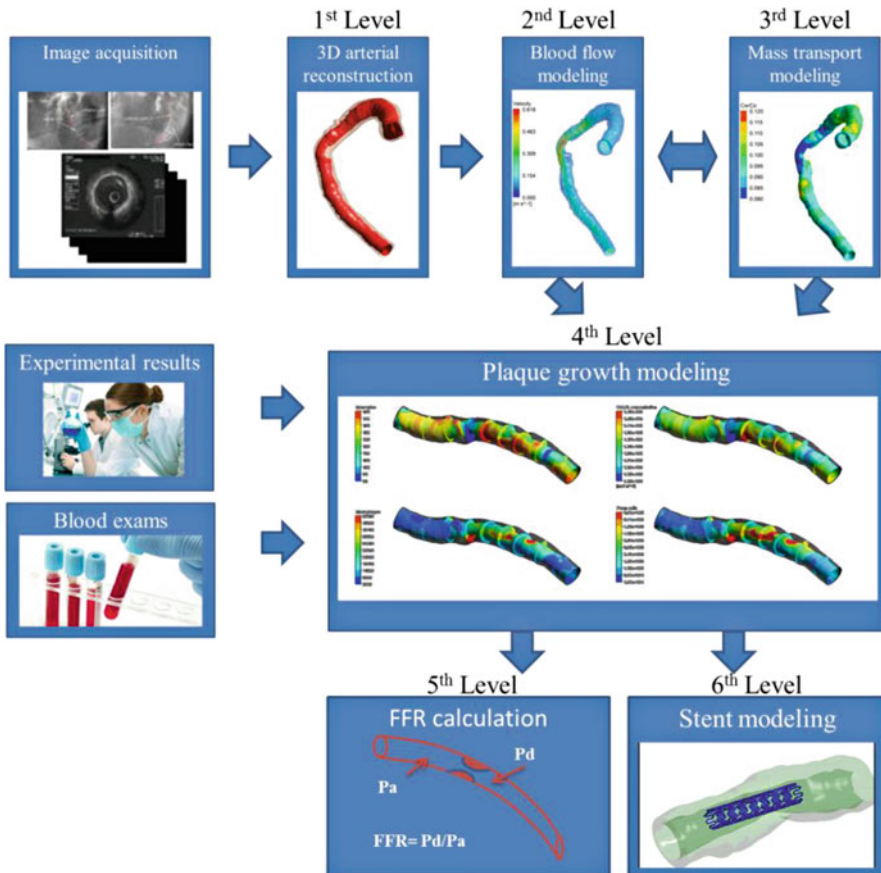

Fig. 1 Multi-level modeling approach of atherosclerotic plaque development

and their accumulation into the arterial wall. In the fourth level, plaque growth is modeled utilizing the results of the previous levels to model the inflammation in the arterial wall and the formation of foam cells. Data from experimental and animal studies have been used for the calculation of the parameters which are applied in the computational models. The fifth level consists of an innovative approach of FFR calculation, while in the sixth level, our stent deployment modeling approach, we studied the performance of the Leader Plus stent type expansion inside a patient specific coronary arterial segment focusing on the arterial stresses in the contact region with the stent.

2   Multi-Level Modeling of Atherosclerosis

2.1   Level 1: 3D Arterial Reconstruction Using Medical Images

The prerequisite of the modeling approaches which employ the finite element method is the use of geometries which represent the physical domain. Accurate modeling of biomechanical systems requires realistic description of the system geometry. Similarly, modeling approaches in atherosclerosis require an accurate representation of the arterial segments or arterial trees. The arteries were reconstructed utilizing various imaging modalities, e.g., intravascular ultrasound (IVUS), angiography, MRI, computed coronary tomography angiography (CCTA). In the following sections, the methodologies for 3D reconstruction of arteries based on the fusion of IVUS and angiography, CT, and MRI are presented.

3D Coronary Artery Reconstruction Using IVUS and Angiography

Coronary artery reconstruction was performed based on the fusion of bi-plane angiography and IVUS data [5]. Briefly, two orthogonal views of angiography are acquired and the catheter path is found. Using the orthogonal views, a 3D catheter path is generated. Active contours are implemented for the automate segmentation of IVUS frames and the detection of the lumen and media-adventitia borders. In the next step, the detected borders are placed perpendicularly onto the 3D catheter path after appropriate absolute orientation of the IVUS frames onto the path. The outcome of this process was two point clouds that represent the luminal and media-adventitia wall geometry.

3D Artery Reconstruction Using MRI

MRI imaging can be used for the imaging and consequently the reconstruction of arteries. Auer et al. introduced an active contour algorithm for the segmentation

of high-resolution MRI and then proposed a methodology that uses statistical information to characterize the plaque components [6]. Adame et al. [7] combined a model-based segmentation algorithm and fuzzy clustering in order to detect the vessel wall, lumen, and lipid core borders. An interesting study was performed by Hofman et al. who used Bayesian, K-Nearest neighbor, feed-forward neural networks, and a combination of Bayes classifier with the Parzen to characterize the type of the plaque in the carotid arteries [8]. Finally, Liu et al. [9] presented a Bayesian approach which used the pixel's intensity, the wall thickness, and the distance from the lumen to characterize plaque composition.

Our methodology includes four main steps [10]: (i) image acquisition and pre-processing of T1-Weighted, and Time-of-Flight (TOF) and T2-Weighted images, (ii) luminal border detection, (iii) outer vessel wall detection, and (iv) characterization of the composition of the plaque (hemorrhages, calcium, lipid cores, and fibrotic plaques). Active contours theory is implemented for lumen and outer vessel wall border detection in TOF and T1-Weighted images, respectively. Moreover, identification of the bifurcation is achieved using the theory of connecting components, while the different plaque types are classified into hemorrhages, calcium, lipid cores, and fibrotic plaques based on a knowledge-based algorithm. Validation of the proposed methodology was made using two experts' annotations (inter-observer variability for the lumen was -1.60 ± 6.70 and for the outer vessel wall was $0.56 \pm 6.28\%$) [10]. Plaque type is also accurately characterized after a validation in 591 images [10].

3D Artery Reconstruction Using CT

Several studies have demonstrated that CCTA provides an accurate analysis of coronary artery remodeling and is able to detect and quantify atherosclerotic plaque [11, 12]. Furthermore, different studies have proved the ability of CCTA to assess plaque burden and classify plaque composition [13]. Voros et al. [14] attempted to validate three-dimensional, quantitative measurements of coronary plaque by CCTA using IVUS. In a similar manner, Graaf et al. [15] correlated the metrics calculated using a fully automated CCTA methodology with those derived by VH-IVUS. Another study for the quantification of coronary arterial stenoses using CCTA was presented by Arbab et al. [16]. This approach indicated that CCTA in comparison with the conventional angiography is able to identify non-invasively patients with coronary artery disease. Recently, Athanasiou et al. [17] presented an innovative three-dimensional reconstruction methodology of coronary arteries and their plaque morphology, using CCTA images.

Our approach includes seven stages (Fig. 2). In the first stage the CCTA images are pre-processed using the Frangi Vesselness filter [18], which identifies tubular structures and limits the region of interest (ROI) to vessel candidate regions. In the second stage, a centerline extraction methodology is applied, using a minimum cost

Fig. 2 The seven stages of the proposed artery reconstruction using CCTA
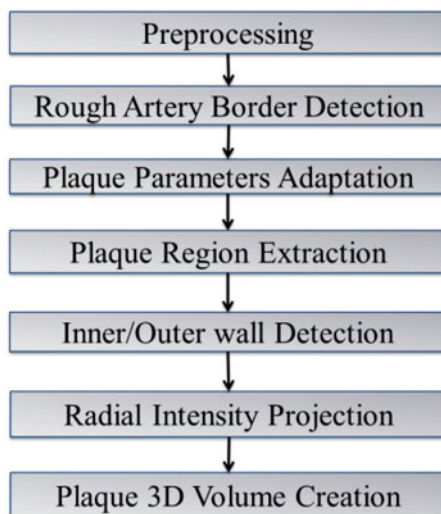
path approach [19]. In the third stage a weight function for lumen, outer wall, and calcified plaque is estimated, based on a membership function of Hounsfield Units (HU) values and the distance from the centerline. This function aims to compensate different protocols for discriminating lumen, outer wall, and calcified plaque. In the fourth stage, an extension of active contour models [20] for lumen segmentation is implemented. In the fifth stage, similar to the previous stage, a level set approach for outer wall segmentation is implemented. This approach uses as a prior shape for the outer wall the previously segmented lumen. In the sixth stage, a level set method is applied for plaque segmentation, taking into consideration calcium objects of significant size. Finally, in the seventh stage the 3D surfaces for the lumen, outer wall, and the calcified plaques are constructed.

2.2 Level 2: Blood Flow Modeling

Hemodynamics and especially, shear stress, found to play a considerable role in the development of atherosclerotic plaques [2]. Blood flow is modeled using the Navier–Stokes equations. The solution of the Navier–Stokes equations requires appropriate boundary conditions and in the case of the transient simulation initial conditions are also needed. We assume that the blood flow is laminar and incompressible. In addition the blood is considered to be Newtonian or non-Newtonian. The arterial wall is assumed to be rigid and non-deformable. The inflow boundary condition is defined by a constant velocity profile or a constant mass flow rate while at the outlet of the arterial segment we define a constant average pressure

profile. Finally, at the fixed walls all velocity components are set to be zero (no-slip boundary condition). In the case of transient flow the inflow is defined by the volumetric blood flow rate or a time dependent velocity profile. The flow rate is specified by a waveform, while three cardiac cycles are required as a general rule for accurate solution of pulsatile simulations. Blood flow modeling has been performed in several studies using mainly the finite element method [21–24]. Papafaklis et al. [25] studied the hemodynamics in coronary arteries bifurcation and investigated the influence of ESS to arterial wall thickening.

The ESS calculation is associated with the arterial geometry especially for regions of increased stenosis [26]. The presence of stenosis has a dramatic effect on the local ESS distribution, while tachycardia had a pronounced impact on ESS in the region of a stenosis with 3–5.7 fold decrease in time-averaged values during one cardiac cycle, compared to the normal heart rate profile [26]. ESS is also correlated with neointima formation after stent implantation [27]. In particular, in patients with bare metal stents (BMS) a negative association was noted between ESS and neointima burden ($p = 0.002$) as well as between ESS and the percentage of the neointimal necrotic core component ($p = 0.015$). In patients with biolimus eluting stents (BES), the suppression of neointimal formation did not allow evaluation of the effect of ESS on its tissue characteristics. Thus, ESS determines not only the amount but also the composition of the neointima in BMS. In the PROSPECT-CT study it was found that CCTA-derived variables had a moderate accuracy in detecting lesions that are likely to progress at follow-up [28]. Performing simulations at 17 bifurcations of the PROSPECT-CT database [29], we found that the Murray's law [30] provides the best accuracy to predict disease progression and also that the use of the side branch in the calculations of ESS is necessary for accurate results. More specifically, low ESS is an independent predictor of lumen reduction and necrotic core increase.

2.3 Level 3: LDL Transport Modeling

The third level is the modeling of LDL transport and its accumulation in the arterial wall. The same principles apply for the HDL transport as well as other cells transport such as monocytes. The rationale is that LDL is transferred in the arterial lumen not only by the blood flow (convection) but also by diffusion due to the concentration difference. Furthermore, LDL/HDL molecules penetrate the endothelial membrane and accumulate into the arterial wall. In order to model macromolecular transport in arteries the convection-diffusion equation is employed.

Prosi et al. [31] have classified mass transfer models into three major categories: (a) the wall-free models, (b) the lumen-wall models, and (c) the multi-layer models. In wall-free models the arterial wall is non-permeable and the wall thickness is not taken into account. Hong et al. [32] presented a numerical simulation of pulsatile flow and macromolecular transport in complex blood vessels. The arterial wall was assumed rigid and the low density lipoprotein (LDL) molecule was too large to penetrate the arterial wall. The lumen-wall models are a more realistic approach since the transport within the lumen is coupled with that in the arterial wall. In these models, the arterial wall is simplified as a homogeneous porous monolayer. Sun et al. [33] and Olgac et al. [34] investigated the influence of the ESS on the arterial mass transport by modeling the blood flow and the solute transport in the lumen and the arterial wall. The most realistic models are the multilayer models, in which the arterial wall consists of more than one layers. Mass transport is made in each layer and interaction between these layers exists. Prosi et al. [31] introduced several mathematical models, based on partial differential equations, to study the coupled transport of macromolecules in the blood stream and in the arterial wall.

We have implemented two LDL transport models. The first one has been proposed by Sun et al. [35]. The second approach enhances the effect of LDL accumulation in the luminal side assuming that endothelial permeability increases when the local luminal LDL concentration is high [26]. Finally, another approach has also been developed which describes a permeability model based on the local endothelial dysfunction caused by the expression of nitric oxide [36]. Results of these studies are summarized below. The endothelial permeability is modeled assuming that the endothelium is a semi-permeable biological membrane. The Kedem–Katchalsky equations [37] are employed. The permeability term of these equations is of utmost importance and several experiments and studies attempted to define it [38]. However, pathological conditions such as hypertension or diabetes could increase endothelial permeability. Besides the constant endothelial permeability model, a variable permeability model which depends on the local luminal LDL concentration [39] has been developed.

Regarding the LDL transport modeling, we showed in one coronary artery that hypertension and tachycardia affect LDL accumulation [26]. The model of endothelial permeability which is based on the local LDL concentration showed that the clinical impact of LDL in real life is simulated more accurately with this model. LDL transport modeling was implemented in large arterial datasets in order to show LDL's effect to plaque growth using baseline and retrospective imaging data. The results show that there is a correlation of high LDL accumulation with plaque growth and especially with plaque burden increase. This finding is observed first in 58 coronary arteries acquired from the PROSPECT database [40]. It was also shown using a dataset of 12 carotid arteries where for the first time MRI examinations from three time points are used [41]. However, the accuracy to predict regions of plaque growth is similar with low ESS leading us to use more sophisticated LDL transport models, as the one based on the local luminal LDL concentration or the proposed endothelial dysfunction model which is based on the production of nitric oxide.

2.4   Level 4: Plaque Growth Modeling

The fourth level of multi-level modeling of atherosclerotic plaque growth is the modeling of the major mechanisms which underlie the initiation and the formation of plaque into the arterial wall. The first two studies were presented by Filipovic et al. [42] and Parodi et al. [43]. Another plaque growth model was presented by Cilla et al. [44]. It was applied in an artificial axisymmetric geometrical coronary artery model. The results though it was not implemented into realistic arteries show that the presented model can simulate the atheromatic plaque growth despite the use of an artificial geometry.

In this level, we first model the oxidation of LDL. It is the first time that such a model for the atheroprotective effect of HDL in the oxidation of LDL has been presented. Thus, experimental data are used to develop a novel LDL oxidation model [45]. In the next step, the effect of cytokines, the transport of monocytes and their differentiation to macrophages, and finally the absorption of oxidized LDL by them to form the foam cells are simulated [46]. The computational model has been implemented in proof-of-concept studies of animal or human data recruited during the ARTREAT project or using data from the databases of PROSPECT and IBIS studies. The first version of the model includes only the modeling of the LDL oxidation. More specifically, we assume that LDL is oxidized when it gets inside the arterial wall. However, this mechanism is affected by the existence of local concentration of HDL which plays an atheroprotective role to plaque development. The proposed model was based on experimental studies. The model was implemented in an arterial segment using pig data [47] and the results have shown that the calculated oxidized concentration of LDL correlates well with the lipid plaque components found in histological images. In the most complex form of the plaque growth model, we model monocytes migration but also their differentiation to macrophages into the arterial wall to finally estimate the formation of foam cells. This model has been implemented in human arteries (coronaries and carotids). In both cases the major conclusion is that advanced modeling of plaque growth is necessary to increase the accuracy to predict the regions which are prone for disease progression. More specifically, in the carotid artery we found that the oxidized LDL and macrophages are correlated with lumen reduction and thickness change, while the prediction accuracy of using all calculated variables in a multi-variate model increases against of using only the low ESS as a predictor of disease progression [48]. In a recent proof-of-concept case we demonstrated a validation scenario of plaque growth modeling using follow-up virtual histology IVUS and optical coherence tomography data from a human coronary arterial segment. In this case the prediction accuracy is over 75% when using all variables [46]. The overall multi-level approach results are shown in Fig. 3.
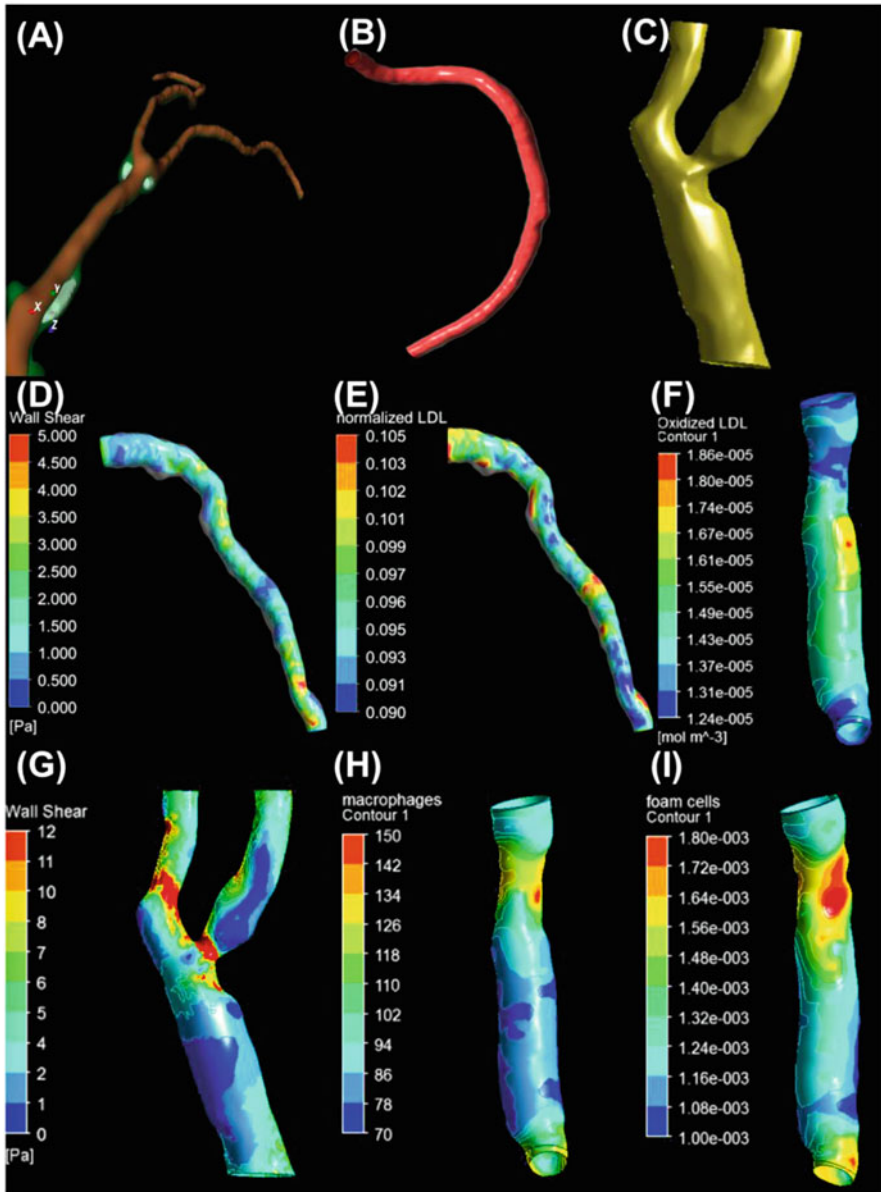
Fig. 3 Multi-level rationale of plaque growth modeling. (**A–C**) 3D reconstruction of coronary and carotid arteries, (**D**, **G**) ESS distribution coronary and carotid artery, (**E**) LDL accumulation in the arterial wall in the LDL transport modeling level, and (**F**, **H**, **I**) oxidized LDL, macrophages, and foam cells accumulation in the arterial wall in plaque growth modeling level

2.5   Level 5: Computational Prediction of FFR

Fractional Flow Reserve (FFR) is considered the gold standard in every day clinical practice for the evaluation of the severity of coronary lesions. However, it requires the use of a dedicated pressure-flow wire, thus increasing the total cost of the whole examination, as well as the discomfort of the patient. In order to tackle this issue, several approaches have been reported in literature that combine non-invasive imaging techniques (CCTA) and the use of computational fluid dynamics to provide an estimation of the invasively measured FFR [49, 50]. Virtual functional assessment index (vFAI) has been proposed as an accurate and valid equivalent to the invasively measured FFR, allowing the evaluation of the hemodynamic status of an existing coronary lesion in short time. Our method utilizes three-dimensional (3D) anatomical data from the coronary vasculature and performs blood flow modeling to calculate the ratio of pressures distal and proximal over the lesion for flows ranging from 0 to 4 mL/s, normalized by the same ratio for a totally healthy artery, offering an insight in CAD hemodynamic significance that is numerically equal to the invasively measured FFR. In coronary angiography derived 3D models, close correlation ($r = 0.78$, $p < 0.0001$) and agreement of vFAI compared to wire-FFR (mean difference: -0.0039 ± 0.085, $p = 0.59$) was found [51]. Diagnostic accuracy, sensitivity, and specificity for the optimal vFAI cut-point (≤ 0.82) were 88%, 90%, and 86%, respectively. Regarding CCTA derived 3D models, very good correlation ($r = 0.88$, $p < 0.001$) and strong agreement between vFAI and invasively measured FFR (mean difference: -0.0039 ± 0.04) were also found [52]. The respective diagnostic accuracy, sensitivity, and specificity for the optimal vFAI cut-point (≤ 0.84) were 91.7%, 75%, and 96.4%. Finally, in hybrid IVUS-angiography 3D models, a modest correlation ($r = 0.84$, $p = 0.073$) was found [53].

2.6   Level 6: Stent Modeling

Computational simulations might be an effective tool for investigating the mechanical performance of stents and evaluating the arterial implications such as in stent restenosis coming from different stent designs and materials, a process that cannot be fully assessed in experimental studies [54]. Towards this direction, several research teams have provided valuable information, either by performing computational simulations of stent deployment inside idealized arteries, or even utilizing patient specific imaging data for the reconstruction of arterial segments [55, 56].

The unexpanded configuration of the 3D finite element model consisted of one 3D reconstructed coronary arterial segment and the Leader Plus stent geometry (Fig. 4). The mesh was created with 3D higher order ten node elements. The mesh sensitivity was implemented with a convergence criterion of the maximum von Mises stresses being within 5%. Stent deployment was performed following a
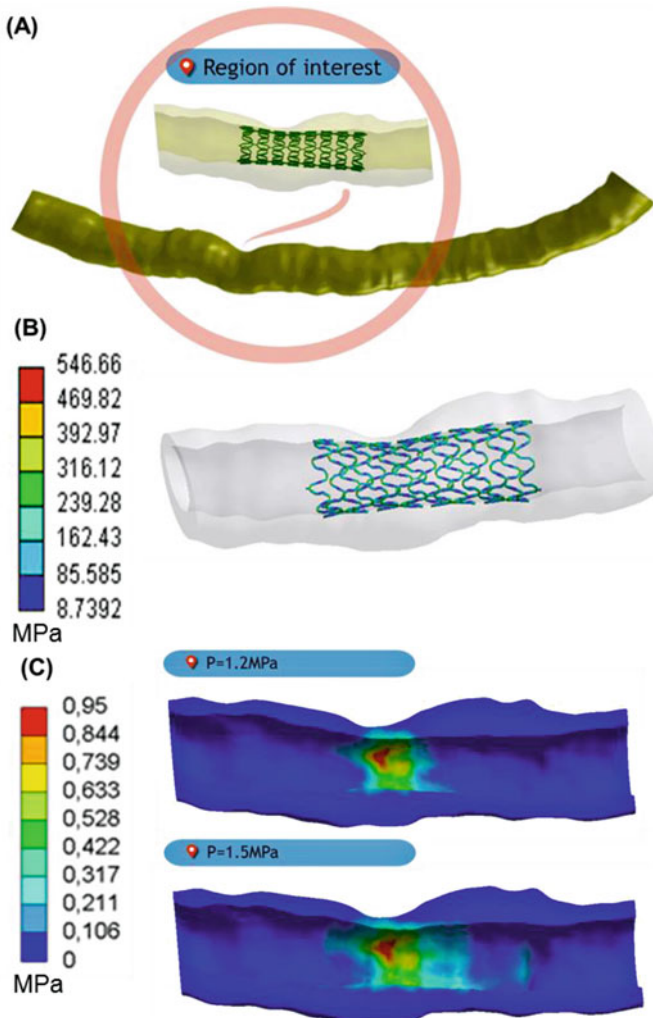
Fig. 4 (**a**) The reconstructed artery and the LeaderPlus stent. (**b**) Von Mises stress distribution in the deformed Leader Plus Stent. (**c**) Von Mises stress at the arterial wall (MPa) during stent expansion for the applied pressure of 1.2 MPa and 1.5 MPa

pressure driven approach through the application of a pressure directly to the inner stent surface. To represent the performance of the human tissue, several material models can be utilized. In our model, the artery was assumed homogeneous with nonlinear behavior. A polynomial form of the Mooney–Rivlin hyperelastic material model was used for the arterial wall [57], with the strain energy density function based on Maurel et al. [58], whereas a bilinear elasto-plastic material model was employed for the stent. The stent was initially placed in the arterial stenosis region.

The ends of the artery were not allowed to move or rotate, appropriate boundary conditions allowed the movement in the axial and radial directions of the stent, whereas stent inflation was enabled by a pressure of 1.5 MPa. Stent expansion was achieved under uniform pressure, however, due to the asymmetry of the stenosed arterial region, stent struts deformed non-uniformly (Fig. 4). The investigation of the stent response is of great importance since high stent stresses can result in stent fracture and consequently in arterial injury. High stresses, approximately 550 MPa, were observed in the stent connectors. During stent deployment, the von Mises stresses were increasing (Fig. 4) and high von Mises stresses occurred in the arterial-stent surface.

3   Discussion and Conclusions

A methodological approach for the computational modeling of the major mechanisms of atherosclerotic plaque development has been presented in this work. Until recently 3D reconstruction and blood flow were only utilized to estimate disease progression. In the current work we propose a multi-level modeling scheme consisting of the 3D reconstruction level, the blood flow modeling and ESS estimation level, the LDL transport modeling level, the plaque growth modeling level but also the stent deployment modeling. Regarding the level of blood flow modeling, first, we prove the effect of geometry and existed stenosis to ESS distribution as well as the effect of tachycardia and hypertension. Second, we associate ESS with disease progression utilizing the CT imaging modality and for the first time we prove that CT imaging can accurately be used for the calculation of ESS and disease progression. Third, for the first time we present an analysis of ESS and neointima formation in arterial segments with deployed stent. Going beyond the state of the art in LDL transport modeling we presented several novel models for endothelial permeability as well as different analyses of the effect of LDL concentration at plaque progression. More specifically, we developed a model of endothelial permeability and LDL transport which is based on the local concentration of LDL concentration. The developed model has been applied to different datasets of arteries demonstrating the ability to predict regions which are prone for plaque growth.

The major innovation is the development of plaque growth computational models. This work starts with the development of an LDL oxidation model. The proposed LDL oxidation model is based not only on the LDL accumulation in the arterial wall, but also on the HDL concentration which has an atheroprotective role on disease progression. The last part is the development of a plaque growth model which simulates the major mechanisms of the atherosclerotic plaque growth process. These mechanisms beside the LDL oxidation are the migration of monocytes into the arterial wall under the effect of cytokines expression and their consequent transformation to macrophages. The appearance of macrophages into the arterial wall with the existence of oxidized LDL leads to the formation of foam cells.

In this model we included all these mechanisms. We applied the proposed model in several cases (one carotid artery and three coronary arteries) and the comparison of the simulation results with the retrospective follow-up data prove that our model is highly promising for a new kind of thinking in the field of atherosclerotic plaque development. More specifically, until now low ESS is considered as a predictor of disease progression without, however, accurate results. Complex modeling of plaque growth increases the accuracy of disease prediction.

References

1. Libby P, Ridker PM, Hansson GK (2011) Progress and challenges in translating the biology of atherosclerosis. Nature 473(7347):317–325
2. Chatzizisis YS, Coskun AU, Jonas M, Edelman ER, Feldman CL, Stone PH (2007) Role of endothelial shear stress in the natural history of coronary atherosclerosis and vascular remodeling – molecular, cellular, and vascular behavior. J Am Coll Cardiol 49(25):2379–2393
3. Chien S (2003) Molecular and mechanical bases of focal lipid accumulation in arterial wall. Prog Biophys Mol Biol 83(2):131–151
4. Surdell D, Shaibani A, Bendok B, Eskandari MK (2007) Fracture of a nitinol carotid artery stent that caused restenosis. J Vasc Interv Radiol 18(10):1297–1299
5. Bourantas CV, Kalatzis FG, Papafaklis MI, Fotiadis DI, Tweddel AC, Kourtis IC, Katsouras CS, Michalis LK (2008) ANGIOCARE: an automated system for fast three-dimensional coronary reconstruction by integrating angiographic and intracoronary ultrasound data. Catheter Cardiovasc Interv 72(2):166–175
6. Auer M, Stollberger R, Regitnig P, Ebner F, Holzapfel GA (2006) 3-D reconstruction of tissue components for atherosclerotic human arteries using ex vivo high-resolution MRI. IEEE Trans Med Imaging 25(3):345–357
7. Adame IM, van der Geest RJ, Wasserman BA, Mohamed MA, Reiber JH, Lelieveldt BP (2004) Automatic segmentation and plaque characterization in atherosclerotic carotid artery MR images. MAGMA 16(5):227–234
8. Hofman JM, Branderhorst WJ, ten Eikelder HM, Cappendijk VC, Heeneman S, Kooi ME, Hilbers PA, ter Haar Romeny BM (2006) Quantification of atherosclerotic plaque components using in vivo MRI and supervised classifiers. Magn Reson Med 55(4):790–799
9. Liu F, Xu D, Ferguson MS, Chu B, Saam T, Takaya N, Hatsukami TS, Yuan C, Kerwin WS (2006) Automated in vivo segmentation of carotid plaque MRI with morphology-enhanced probability maps. Magn Reson Med 55(3):659–668
10. Sakellarios AI, Stefanou K, Siogkas P, Tsakanikas VD, Bourantas CV, Athanasiou L, Exarchos TP, Fotiou E, Naka KK, Papafaklis MI, Patterson AJ, Young VE, Gillard JH, Michalis LK, Fotiadis DI (2012) Novel methodology for 3D reconstruction of carotid arteries and plaque characterization based upon magnetic resonance imaging carotid angiography data. Magn Reson Imaging 30(8):1068–1082
11. Papadopoulou S-L, Neefjes LA, Schaap M, Li H-L, Capuano E, van der Giessen AG, Schuurbiers JCH, Gijsen FJH, Dharampal AS, Nieman K, van Geuns RJ, Mollet NR, de Feyter PJ (2011) Detection and quantification of coronary atherosclerotic plaque by 64-slice multidetector CT: a systematic head-to-head comparison with intravascular ultrasound. Atherosclerosis 219(1):163–170

12. Divakaran S, Cheezum M, Hulten E, Bittencourt M, Silverman M, Nasir K, Blankstein R (2015) Use of cardiac CT and calcium scoring for detecting coronary plaque: implications on prognosis and patient management. Br J Radiol 88(1046):20140594

13. Saremi F, Achenbach S (2015) Coronary plaque characterization using CT. Am J Roentgenol 204(3):W249–W260

14. Voros S, Rinehart S, Qian Z, Vazquez G, Anderson H, Murrieta L, Wilmer C, Carlson H, Taylor K, Ballard W (2011) Prospective validation of standardized, 3-dimensional, quantitative coronary computed tomographic plaque measurements using radiofrequency backscatter intravascular ultrasound as reference standard in intermediate coronary arterial lesions: results from the ATLANTA (assessment of tissue characteristics, lesion morphology, and hemodynamics by angiography with fractional flow reserve, intravascular ultrasound and virtual histology, and noninvasive computed tomography in atherosclerotic plaques) I study. J Am Coll Cardiol Intv 4(2):198–208

15. de Graaf MA, Broersen A, Kitslaar PH, Roos CJ, Dijkstra J, Lelieveldt BP, Jukema JW, Schalij MJ, Delgado V, Bax JJ (2013) Automatic quantification and characterization of coronary atherosclerosis with computed tomography coronary angiography: cross-correlation with intravascular ultrasound virtual histology. Int J Card Imaging 29(5):1177–1190

16. Arbab-Zadeh A, Hoe J (2011) Quantification of coronary arterial stenoses by multidetector CT angiography in comparison with conventional angiography methods, caveats, and implications. J Am Coll Cardiol Img 4(2):191–202

17. Athanasiou L, Rigas G, Sakellarios AI, Exarchos TP, Siogkas PK, Bourantas CV, Garcia-Garcia HM, Lemos PA, Falcao BA, Michalis LK (2016) Three-dimensional reconstruction of coronary arteries and plaque morphology using CT angiography–comparison and registration with IVUS. BMC Med Imaging 16(1):1

18. Frangi AF, Niessen WJ, Vincken KL, Viergever MA (1998) Multiscale vessel enhancement filtering. In: Wells WM, Colchester A, Delp S (eds) Medical image computing and computer-assisted intervention — MICCAI'98: first international conference Cambridge, MA, USA, October 11–13, 1998 proceedings. Springer, Berlin Heidelberg, pp 130–137. doi:10.1007/BFb0056195

19. Metz C, Schaap M, Weustink A, Mollet N, van Walsum T, Niessen W (2009) Coronary centerline extraction from CT coronary angiography images using a minimum cost path approach. Med Phys 36(12):5568–5579

20. Chan TF, Vese LA (2001) Active contours without edges. IEEE Trans Image Process 10(2):266–277

21. Taylor CA, Steinman DA (2010) Image-based modeling of blood flow and Vessel Wall dynamics: applications, methods and future directions. Ann Biomed Eng 38(3):1188–1203

22. Saad Y, Schultz MH (1986) Gmres – a generalized minimal residual algorithm for solving nonsymmetric linear-systems. SIAM J Sci Stat Comput 7(3):856–869

23. Perktold K, Hofer M, Rappitsch G, Loew M, Kuban BD, Friedman MH (1998) Validated computation of physiologic flow in a realistic coronary artery branch. J Biomech 31(3):217–228

24. Steinman DA, Thomas JB, Ladak HM, Milner JS, Rutt BK, Spence JD (2002) Reconstruction of carotid bifurcation hemodynamics and wall thickness using computational fluid dynamics and MRI. Magn Reson Med 47(1):149–159

25. Papafaklis MI, Vergallo R, Jia HB, Bourantas C, Yonetsu T, Lakkas L, McNulty I, Kotsia A, Lee H, Antoniadis A, Yu B, Naka KK, Fotiadis DI, Feldman C, Michalis L, Jang IK, Stone P (2013) Longitudinal distribution of endothelial shear stress along culprit lesions and association with plaque characteristics in patients with acute coronary syndromes: a three-dimensional frequency-domain optical coherence tomography study. J Am Coll Cardiol 62(18):B198–B198

26. Sakellarios AI, Papafaklis MI, Siogkas P, Athanasiou LS, Exarchos TP, Stefanou K, Bourantas CV, Naka KK, Michalis LK, Parodi O, Fotiadis DI (2013) Patient-specific computational modeling of subendothelial LDL accumulation in a stenosed right coronary artery: effect of hemodynamic and biological factors. Am J Physiol Heart C 304(11):H1455–H1470

27. Bourantas CV, Raber L, Zaugg S, Sakellarios A, Taniwaki M, Heg D, Moschovitis A, Radu M, Papafaklis MI, Kalatzis F, Naka KK, Fotiadis DI, Michalis LK, Serruys PW, Garcia Garcia HM, Windecker S (2015) Impact of local endothelial shear stress on neointima and plaque following stent implantation in patients with ST-elevation myocardial infarction: a subgroup-analysis of the COMFORTABLE AMI-IBIS 4 trial. Int J Cardiol 186:178–185

28. Bourantas CV, Papadopoulou SL, Serruys PW, Sakellarios A, Kitslaar PH, Bizopoulos P, Girasis C, Zhang YJ, de Vries T, Boersma E, Papafaklis MI, Naka KK, Fotiadis DI, Stone GW, Reiber JH, Michalis LK, de Feyter PJ, Garcia-Garcia HM (2015) Noninvasive prediction of atherosclerotic progression: the PROSPECT-MSCT study. JACC Cardiovasc Imaging 9(8):1009–1011

29. Papadopoulou SL, Neefjes LA, Garcia-Garcia HM, Flu WJ, Rossi A, Dharampal AS, Kitslaar PH, Mollet NR, Veldhof S, Nieman K, Stone GW, Serruys PW, Krestin GP, de Feyter PJ (2012) Natural history of coronary atherosclerosis by multislice computed tomography. JACC Cardiovasc Imag 5(3):S28–S37

30. Murray CD (1926) The physiological principle of minimum work applied to the angle of branching of arteries. J Gen Physiol 9(6):835–841

31. Prosi M, Zunino P, Perktold K, Quarteroni A (2005) Mathematical and numerical models for transfer of low-density lipoproteins through the arterial walls: a new methodology for the model set up with applications to the study of disturbed lumenal flow. J Biomech 38(4):903–917

32. Hong J, Wei L, Fu C, Tan W (2008) Blood flow and macromolecular transport in complex blood vessels. Clin Biomech 23(Suppl 1):S125–S129

33. Sun N, Wood NB, Hughes AD, Thom SA, Xu XY (2006) Fluid-wall modelling of mass transfer in an axisymmetric stenosis: effects of shear-dependent transport properties. Ann Biomed Eng 34(7):1119–1128

34. Olgac U, Knight J, Poulikakos D, Saur SC, Alkadhi H, Desbiolles LM, Cattin PC, Kurtcuoglu V (2011) Computed high concentrations of low-density lipoprotein correlate with plaque locations in human coronary arteries. J Biomech 44(13):2466–2471

35. Sun N, Wood NB, Hughes AD, Thom SAM, Xu XY (2006) Fluid-wall modelling of mass transfer in an axisymmetric stenosis: effects of shear-dependent transport properties. Ann Biomed Eng 34(7):1119–1128

36. Sakellarios AI, Siogkas P, Exarchos T, Stefanou K, Bourantas CV, Athanasiou L, Fotiou E, Papafaklis M, Naka KK, Michalis LK, Fotiadis DI (2011) Modelling LDL accumulation in the case of endothelial dysfunction. J Serbian Soc Comput Mech 5(2):90–100

37. Kedem O, Katchalsky A (1958) Thermodynamic analysis of the permeability of biological membranes to non-electrolytes. Biochim Biophys Acta 27(2):229–246

38. Stangeby DK, Ethier CR (2002) Coupled computational analysis of arterial LDL transport – effects of hypertension. Comput Methods Biomech Biomed Engin 5(3):233–241

39. Guretzki HJ, Gerbitz KD, Olgemoller B, Schleicher E (1994) Atherogenic levels of low density lipoprotein alter the permeability and composition of the endothelial barrier. Atherosclerosis 107(1):15–24

40. Sakellarios A, Bourantas CV, Papadopoulou SL, Tsirka Z, de Vries T, Kitslaar PH, Girasis C, Naka KK, Fotiadis DI, Veldhof S, Stone GW, Reiber JH, Michalis LK, Serruys PW, de Feyter PJ, Garcia-Garcia HM (2016) Prediction of atherosclerotic disease progression using LDL transport modelling: a serial computed tomographic coronary angiographic study. Eur Heart J Cardiovasc Imaging 18(1):11–18. doi:10.1093/ehjci/jew035

41. Sakellarios AI, Bizopoulos P, Papafaklis MI, Athanasiou L, Exarchos T, Bourantas CV, Naka KK, Patterson AJ, Young VE, Gillard JH, Parodi O, Michalis LK, Fotiadis DI (2016) Natural history of carotid atherosclerosis in relation to the hemodynamic environment: a low-density lipoprotein transport modeling study with serial magnetic resonance imaging in humans. Angiology 68(2). doi:10.1177/0003319716644138

42. Filipovic N, Nikolic D, Saveljic I, Milosevic Z, Exarchos T, Pelosi G, Parodi O (2013) Computer simulation of three-dimensional plaque formation and progression in the coronary artery. Comput Fluids 88:826–833

43. Siogkas P, Sakellarios A, Exarchos TP, Athanasiou L, Karvounis E, Stefanou K, Fotiou E, Fotiadis DI, Naka KK, Michalis LK, Filipovic N, Parodi O (2011) Multiscale – patient-specific artery and atherogenesis models. IEEE T Biomed Eng 58(12):3464–3468

44. Cilla M, Pena E, Martinez MA (2014) Mathematical modelling of atheroma plaque formation and development in coronary arteries. J R Soc Interface 11(90):1–16

45. Kunitake ST, Jarvis MR, Hamilton RL, Kane JP (1992) Binding of transition-metals by apolipoprotein-a-I-containing plasma-lipoproteins-inhibition of oxidation of low-density lipoproteins. In: Proceedings of the National Academy of Sciences of the United States of America, 1992. pp 6993-6997

46. Sakellarios A, Raeber L, Bourantas C, Exarchos T, Athanasiou L, Pelosi G, Parodi O, Koskinas K, Naka K, Michalis L, Serruys PW, Garcia-Garcia H, Windecker S, Fotiadis D (2016) Prediction of atherosclerotic plaque development in an in vivo coronary arterial segment based on a multi-level modeling approach. IEEE Trans Biomed Eng. doi:10.1109/TBME.2016.2619489

47. Puccinelli E, Gervasi PG, Trivella MG, Vornoli A, Viglione F, Pelosi G, Parodi O, Sampietro T, Puntoni M (2015) Modulation of lipid homeostasis in response to continuous or intermittent high-fat diet in pigs. Animal 9(6):1000–1007

48. Sakellarios AI, Bizopoulos P, Stefanou K, Athanasiou LS, Papafaklis MI, Bourantas CV, Naka KK, Michalis LK, Fotiadis DI (2015) A proof-of-concept study for predicting the region of atherosclerotic plaque development based on plaque growth modeling in carotid arteries. Conf Proc IEEE Eng Med Biol Soc 2015:6552–6555

49. Koo BK, Erglis A, Doh JH, Daniels DV, Jegere S, Kim HS, Dunning A, DeFrance T, Lansky A, Leipsic J, Min JK (2011) Diagnosis of ischemia-causing coronary stenoses by noninvasive fractional flow reserve computed from coronary computed tomographic angiograms. Results from the prospective multicenter DISCOVER-FLOW (diagnosis of ischemia-causing stenoses obtained via noninvasive fractional flow reserve) study. J Am Coll Cardiol 58(19):1989–1997

50. Kruk M, Wardziak L, Demkow M, Pleban W, Pregowski J, Dzielinska Z, Witulski M, Witkowski A, Ruzyllo W, Kepka C (2016) Workstation-based calculation of CTA-based FFR for intermediate stenosis. JACC Cardiovasc Imaging 9(6):690–699

51. Papafaklis MI, Muramatsu T, Ishibashi Y, Lakkas LS, Nakatani S, Bourantas CV, Ligthart J, Onuma Y, Echavarria-Pinto M, Tsirka G, Kotsia A, Nikas DN, Mogabgab O, van Geuns RJ, Naka KK, Fotiadis DI, Brilakis ES, Garcia-Garcia HM, Escaned J, Zijlstra F, Michalis LK, Serruys PW (2014) Fast virtual functional assessment of intermediate coronary lesions using routine angiographic data and blood flow simulation in humans: comparison with pressure wire – fractional flow reserve. EuroIntervention 10(5):574–583

52. Siogkas PK, Anagnostopoulos CD, Exarchos TP, Liga R, Knuuti J, Scholte AJHA, Papafaklis MI, Parodi O, Michalis LK, Neglia D, Fotiadis DI (2016) Computational Hemodynamic Assessment of coronary lesions from Computed Tomography Angiography. A novel approach. In: ESC Congress 2016, Rome, Italy

53. Siogkas PK, Athanasiou LS, Sakellarios AI, Stefanou KA, Exarchos TP, Papafaklis MI, Naka KK, Parodi O, Michalis LK, Fotiadis DI (2015) Validation study of a 3D-QCA coronary reconstruction method using a hybrid intravascular ultrasound and angiography reconstruction method and patient-specific fractional flow reserve data. Conf Proc IEEE Eng Med Biol Soc 2015:973–976

54. Azaouzi M, Makradi A, Petit J, Belouettar S, Polit O (2013) On the numerical investigation of cardiovascular balloon-expandable stent using finite element method. Comput Mater Sci 79:326–335

55. Gervaso F, Capelli C, Petrini L, Lattanzio S, Di Virgilio L, Migliavacca F (2008) On the effects of different strategies in modelling balloon-expandable stenting by means of finite element method. J Biomech 41(6):1206–1212

56. Karanasiou GS, Sakellarios AI, Tripoliti EE, Petrakis EGM, Zervakis ME, Migliavacca F, Dubini G, Dordoni E, Michalis LK, Fotiadis DI (2013) Modeling of stent implantation in a human stenotic artery. In: LMR R (ed) XIII mediterranean conference on medical and biological engineering and computing, Seville, Spain, 2013. Springer International Publishing, Cham, pp 1045–1048

57. Lally C, Reid AJ, Prendergast PJ (2004) Elastic behavior of porcine coronary artery tissue under uniaxial and equibiaxial tension. Ann Biomed Eng 32(10):1355–1364
58. Maurel W (1998) Biomechanical models for soft tissue simulation. ESPRIT basic research series, vol 18155. Springer, Berlin, New York